Aqueous Dispersions of Single-wall and Multiwall Carbon Nanotubes with Designed Amphiphilic Polycations

ARTICLE *in* JOURNAL OF THE AMERICAN CHEMICAL SOCIETY · APRIL 2005

Impact Factor: 12.11 · DOI: 10.1021/ja045670+ · Source: PubMed

8 AUTHORS, INCLUDING:

Kai Sun
University of Michigan
196 PUBLICATIONS **4,005** CITATIONS
SEE PROFILE

James P Wicksted
Oklahoma State University - Stillwater
114 PUBLICATIONS **2,267** CITATIONS
SEE PROFILE

Nicholas Kotov
University of Michigan
445 PUBLICATIONS **26,720** CITATIONS
SEE PROFILE

J|A|C|S
ARTICLES
Published on Web 02/19/2005

Aqueous Dispersions of Single-wall and Multiwall Carbon Nanotubes with Designed Amphiphilic Polycations

Vladimir A. Sinani,[†] Muhammed K. Gheith,[§] Alexander A. Yaroslavov,[‡] Anna A. Rakhnyanskaya,[‡] Kai Sun,[||] Arif A. Mamedov,[⊥] James P. Wicksted,[§] and Nicholas A. Kotov*[,†]

Department of Chemical Engineering, University of Michigan, Ann Arbor, Michigan 48109, Department of Chemistry, Lomonosov Moscow State University, 119899 Moscow, Leninskie Gory, Russia, Department of Physics, Oklahoma State University, Stillwater, Oklahoma 74078, Electron Microbeam Analysis Laboratory, University of Michigan, Ann Arbor, Michigan 48109, and Nomadics Inc., 1024 Innovation Parkway, Stillwater, Oklahoma 74074

Received July 19, 2004; E-mail: kotov@umich.edu

Abstract: Poor solubility of single-walled and multiwalled carbon nanotubes (NTs) in water and organic solvents presents a considerable challenge for their purification and applications. Macromolecules can be convenient solubilizing agents for NTs and a structural element of composite materials for them. Several block copolymers with different chemical functionalities of the side groups were tested for the preparation of aqueous NT dispersions. Poly(*N*-cetyl-4-vinylpyridinium bromide-*co*-*N*-ethyl-4-vinylpyridinium bromide-*co*-4-vinylpyridine) was found to form exceptionally stable NT dispersions. It is suggested that the efficiency of macromolecular dispersion agents for NT solubilization correlates with the topological and electronic similarity of polymer−NT and NT−NT interactions in the nanotube bundles. Raman spectroscopy and atomic force and transmission electron microcopies data indicate that the polycations are wrapped around NTs forming a uniform coating 1.0−1.5 nm thick. The ability to wind around the NT originates in the hydrophobic attraction of the polymer backbone to the graphene surface and topological matching. Tetraalkylammonium functional groups in the side chains of the macromolecule create a cloud of positive charge around NTs, which makes them hydrophilic. The prepared dispersions could facilitate the processing of the nanotubes into composites with high nanotube loading for electronic materials and sensing. Positive charge on their surface is particularly important for biological and biomedical applications because it strengthens interactions with negatively charged cell membranes. A high degree of spontaneous bundle separation afforded by the polymer coating can also be beneficial for NT sorting.

1. Introduction

Single-walled and multiwalled carbon nanotubes (NTs) are important structural blocks for preparation of composites with unique optical,[1−3] electrical,[4−8] and mechanical properties.[6,9] A tremendous amount of work is being done on different aspects of carbon nanotube technology such as synthesis, functionalization, and applications ranging from nanoscale electronic and memory devices to molecular sensors.[7,10−13] One of the most significant problems associated with them and especially with single-wall NTs (SWNTs) is the preparation of their stable, uniform, and aggregation-free dispersions. This makes possible both effective purification and processing of NTs into composites[14−20] in ultrastrong membranes equally suitable for space, military, and medical applications.[21,70] Many research groups

[†] Department of Chemical Engineering, University of Michigan.
[‡] Lomonosov Moscow State University.
[§] Oklahoma State University.
[||] Electron Microbeam Analysis Laboratory, University of Michigan.
[⊥] Nomadics Inc.

(1) Carrillo, A.; Swartz, J. A.; Gamba, J. M.; Kane, R. S.; Chakrapani, N.; Wei, B.; Ajayan, P. M. *Nano Letters* **2003**, *3*, 1437−1440.
(2) Dalton, A. B.; Byrne, H. J.; Coleman, J. N.; Curran, S.; Davey, A. P.; McCarthy, B.; Blau, W. *Synthetic Metals* **1999**, *102*, 1176−1177.
(3) Alvaro, M.; Atienzar, P.; Bourdelande, J. L.; Garcia, H. *Chemical Commununications (Cambridge, United Kingdom)* **2002**, 3004−3005.
(4) Ago, H.; Kugler, T.; Cacialli, F.; Petritsch, K.; Friend, R. H.; Salaneck, W. R.; Ono, Y.; Yamabe, T.; Tanaka, K. *Synthetic Metals* **1999**, *103*, 2494−2495.
(5) Martel, R.; Schmidt, T.; Shea, H. R.; Hertel, T.; Avouris, P. *Applied Physics Letters* **1998**, *73*, 2447−2449.
(6) Ajayan, P. M. *Chemical Reviews* **1999**, *99*, 1787−1799.
(7) Tans, S. J.; Devoret, M. H.; Dal, H.; Thess, A.; Smalley, R. E.; Geerligs, L. J.; Dekker, C. *Nature (London)* **1997**, *386*, 474−477.
(8) Venema, L. C.; Wildoer, J. W. G.; Janssen, J. W.; Tans, S. J.; Tuinstra, H. L. J. T.; Kouwenhoven, L. P.; Dekker, C. *Science (Washington, D.C.)* **1999**, *283*, 52−55.
(9) Dresselhaus, M. S., Dresselhaus, G., Eklund, P. C., Eds. *Science of Fullerenes and Carbon Nanotubes*; 1996; p 965.
(10) Saito, R., Dresselhaus, G., Dresselhaus, M. S., Eds. *Physics of Carbon Nanotube*; 1998; p 200.
(11) Tans, S. J.; Verschueren, A. R. M.; Dekker, C. *Nature (London)* **1998**, *393*, 49−52.
(12) Rueckes, T.; Kim, K.; Joselevich, E.; Tseng, G. Y.; Cheung, C. L.; Lieber, C. M. *Science (Washington, D.C.)* **2000**, *289*, 94−97.
(13) Kong, J.; Franklin, N. R.; Zhou, C.; Chapline, M. G.; Peng, S.; Cho, K.; Dailt, H. *Science (Washington, D.C.)* **2000**, *287*, 622−625.
(14) Abatemarco, T.; Stickel, J.; Belfort, J.; Frank, B. P.; Ajayan, P. M.; Belfort, G. *Journal of Physical Chemistry B* **1999**, *103*, 3534−3538.
(15) Yudasaka, M.; Zhang, M.; Jabs, C.; Iijima, S. *Applied Physics A: Materials Science & Processing* **2000**, *71*, 449−451.
(16) Zhao, B.; Hu, H.; Niyogi, S.; Itkis, M. E.; Hamon, M. A.; Bhowmik, P.; Meier, M. S.; Haddon, R. C. *Journal of the American Chemical Society* **2001**, *123*, 11673−11677.

are interested in NT suspensions in water and simple water/organic mixtures because such solvents decrease the toxicity of the composite production and are more environmentally compliant, which will become one of the critical factors determining the commercial viability of the large-scale NT processing.[14]

Several approaches were proposed for the production of aqueous suspensions of NTs. The most common one is the chemical modification of the graphene surface by oxidation[22−25] followed by organic modification with hydrophilic substances.[26,27] However, disruption of the electronic conjugation in NTs associated with formation of new covalent bonds in the graphene sheet is undesirable due to the inevitable deterioration of the unique NT properties. The functionalization of NTs can also be achieved by noncovalent surface coating by low molecular weight surfactants,[28−30] surface wrapping with polymers such as polystyrene sulfonate,[31,32] and hydrolyzed poly(styrene-*alt*-maleic anhydride).[1] The noncovalent absorption of hydrophilic noncharged polymer molecules such as poly(vinylpyrrolidone),[22,33,34] poly(vinyl alcohol),[35] amylose,[36] or poly(ethylene oxide)[37] on NTs and subsequent solubilization was also reported. However, one usually needs very high concentration of polymers to obtain NT dispersions, which is inconvenient for further NT processing into composite materials.

In this paper, we demonstrate a simple method for the preparation of exceptionally stable aqueous suspensions of NTs in mixed water/DMF solvents, which also imparts strong positive charge to NT dispersions. The high efficiency of the polymeric dispersing agent was achieved on the basis of structural optimization of the macromolecule. Similarly to PSS modification,[34] the NT surface here is wrapped with polymer molecules possessing hydrophobic alkyl pendant groups. The hydrophobic part of the chain is bound to the NT surface via hydrophobic and other intermolecular interactions, while the hydrophilic parts provide solubility in polar solvents. The resulting dispersions are positively charged. This is an important feature for the layer-by-layer assembly (LBL) as a method of NT processing into ultrastrong composites and possibly other applications.[21,70] LBL self-assembly allows creation of composites with uniform NT distribution because phase separation is prevented in each adsorption layer.[21] Positively charged NT suspensions make possible further increase of NT loading in the LBL composite by combining them with negatively charged NT suspensions used previously. One should note, that positively charged macromolecules with intrinsically high strength of the backbone are substantially more difficult to find or synthesize than those which are negatively charged. Availability of the positively charged NT dispersions is also important for biological and biomedical applications involving interactions with negatively charged living cells. For instance, positively charged NT surfaces improve adhesion of neurons on suitable substrates[38] and may be used for drug delivery and other interesting biomedical applications.[33] Similar arguments are applicable for the preparation of actuators, artificial muscles,[39] and biological sensing[37,40] based on NT thin films. Additionally, variation of surface charge around NTs is important for the control of the electronic properties of the nanotube composites.[41,42]

2. Experimental Section

2.1. Materials. NTs were produced by several manufacturers. Single-wall nanotubes (SWNT) were obtained from Nanocyl (Namur, Belgium)(Type I); Carbon Nanotechnology Inc. (Houston, TX); Bucky-Pearls Purified NT (Type II); and Southwest Nanotechnologies (Norman, OK) (Type III). According to the manufacturer specifications, the NTs from Nanocyl were partially oxidized and have some amount of carboxyl functionalities. The degree of oxidation is apparently small because their behavior and solubility in typical NT dispersing mixtures did not differ from NTs produced by Carbon Nanotechnology, Inc. and their chemical modification was detectable only by spectroscopic means (Raman scattering). Multiwall carbon nanotubes (MWNTs) were a gift from Nano-Lab (Boston, MA).

All other chemicals, unless otherwise noted, were purchased from Aldrich (St. Louis, MO) and were used without further purification. Deionized water with nominal resistivity higher than 18.2 MΩ cm was produced by Barnstead E-Pure with a reverse osmosis system was used for all chemical procedures. The pH of solutions was adjusted with 0.1 M HCl or 0.1 M NaOH.

2.2. Preparation of NT/Polymer Suspension. The amphiphilic polymer was synthesized according to the following procedure. A poly-

(17) Banerjee, S.; Wong, S. S. *Journal of Physical Chemistry B* **2002**, *106*, 12144−12151.
(18) Dalton, A. B.; Blau, W. J.; Chambers, G.; Coleman, J. N.; Henderson, K.; Lefrant, S.; McCarthy, B.; Stephan, C.; Byrne, H. J. *Synthetic Metals* **2001**, *121*, 1217−1218.
(19) Chen, J.; Rao, A. M.; Lyuksyutov, S.; Itkis, M. E.; Hamon, M.; Hu, H.; Cohn, R. W.; Eklund, P. C.; Colbert, D. T.; Smalley, R. E.; Haddon, R. C. *Journal of Physical Chemistry B* **2001**, *105*, 2525−2528.
(20) Bandow, S.; Rao, A. M.; Williams, K. A.; Thess, A.; Smalley, R. E.; Eklund, P. C. *Journal of Physical Chemistry B* **1997**, *101*, 8839−8842.
(21) Mamedov, A. A.; Kotov, N. A.; Prato, M.; Guldi, D. M.; Wicksted, J. P.; Hirsch, A. *Nature Materials* **2002**, *1*, 190−194.
(22) Liu, J.; Rinzler, A. G.; Dai, H.; Hafner, J. H.; Bradley, R. K.; Boul, P. J.; Lu, A.; Iverson, T.; Shelimov, K.; Huffman, C. B.; Rodriguez-Macias, F.; Shon, Y. S.; Lee, T. R.; Colbert, D. T.; Smalley, R. E. *Science (Washington, D. C.)* **1998**, *280*, 1253−1256.
(23) Zhao, W.; Song, C.; Pehrsson, P. E. *Journal of the American Chemical Society* **2002**, *124*, 12418−12419.
(24) Hiura, H.; Ebbesen, T. W.; Tanigaki, K. *Advanced Materials (Weinheim, Germany)* **1995**, *7*, 275−276.
(25) Mickelson, E. T.; Chiang, I. W.; Zimmerman, J. L.; Boul, P. J.; Lozano, J.; Liu, J.; Smalley, R. E.; Hauge, R. H.; Margrave, J. L. *Journal of Physical Chemistry B* **1999**, *103*, 4318−4322.
(26) Hamon, M. A.; Chen, J.; Hu, H.; Chen, Y.; Itkis, M. E.; Rao, A. M.; Eklund, P. C.; Haddon, R. C. *Advanced Materials (Weinheim, Germany)* **1999**, *11*, 834−840.
(27) Georgakilas, V.; Tagmatarchis, N.; Pantarotto, D.; Bianco, A.; Briand, J. P.; Prato, M. *Chemical Communications (Cambridge, United Kingdom)* **2002**, 3050−3051.
(28) Li, B.; Shi, Z.; Lian, Y.; Gu, Z. *Chemistry Letters* **2001**, 598−599.
(29) Strano, M. S.; Moore, V. C.; Miller, M. K.; Allen, M. J.; Haroz, E. H.; Kittrell, C.; Hauge, R. H.; Smalley, R. E. *Journal of Nanoscience and Nanotechnology* **2003**, *3*, 81−86.
(30) Krstic, V.; Duesberg, G. S.; Muster, J.; Burghard, M.; Roth, S. *Chemistry of Materials* **1998**, *10*, 2338−2340.
(31) O'Connell, M. J.; Boul, P.; Ericson, L. M.; Huffman, C.; Wang, Y.; Haroz, E.; Kuper, C.; Tour, J.; Ausman, K. D.; Smalley, R. E. *Chemical Physics Letters* **2001**, *342*, 265−271.
(32) Schreuder-Gibson, H.; Senecal, K.; Sennett, M.; Samuelson, L.; Huang, Z.; Wen, J.; Li, W.; Ti, Y.; Wang, D.; Yang, S.; Ren, Z.; Sung, C. *Proceedings − Electrochemical Society* **2000**, *2000−12*, 210−221.
(33) Guan, W.; Wu, C.; Lu, H. *Huazhong Keji Daxue Xuebao, Ziran Kexueban* **2002**, *30*, 114−116.
(34) O'Connell, M. J.; Boul, P.; Ericson, L. M.; Huffman, C.; Wang, Y.; Haroz, E.; Kuper, C.; Tour, J.; Ausman, K. D.; Smalley, R. E. *Chemical Physics Letters* **2001**, *342*, 265−271.
(35) Zhang, X.; Liu, T.; Sreekumar, T. V.; Kumar, S.; Moore, V. C.; Hauge, R. H.; Smalley, R. E. *Nano Letters* **2003**, *3*, 1285−1288.
(36) Kim, O. K.; Je, J.; Baldwin, J. W.; Kooi, S.; Pehrsson, P. E.; Buckley, L. J. *Journal of the American Chemical Society* **2003**, *125*, 4426−4427.
(37) Chen, R. J.; Bangsaruntip, S.; Drouvalakis, K. A.; Kam, N. W. S.; Shim, M.; Li, Y.; Kim, W.; Utz, P. J.; Dai, H. *Proceedings of the National Academy of Sciences of the United States of America* **2003**, *100*, 4984−4989.
(38) Hu, H.; Ni, Y.; Montana, V.; Haddon, R. C.; Parpura, V. *Nano Letters* **2004**, *4*, 507−511.
(39) Gartstein, Y.; Zakhidov, A. A.; Baughman, R. H. *Physical Review Letters* **2002**, *89*, 045503-1-045503/4.
(40) Javey, A.; Guo, J.; Wang, Q.; Lundstrom, M.; Dai, H. *Nature (London, United Kingdom)* **2003**, *424*, 654−657.
(41) Zhang, J.; Lee, J. K.; Wu, Y.; Murray, R. W. *Nano Letters* **2003**, *3*, 403−407.
(42) Lopez Sancho, M. P.; Munoz, M. C.; Chico, L. *Physical Review B: Condensed Matter and Materials Physics* **2001**, *63*, 165419-1-165419/7.

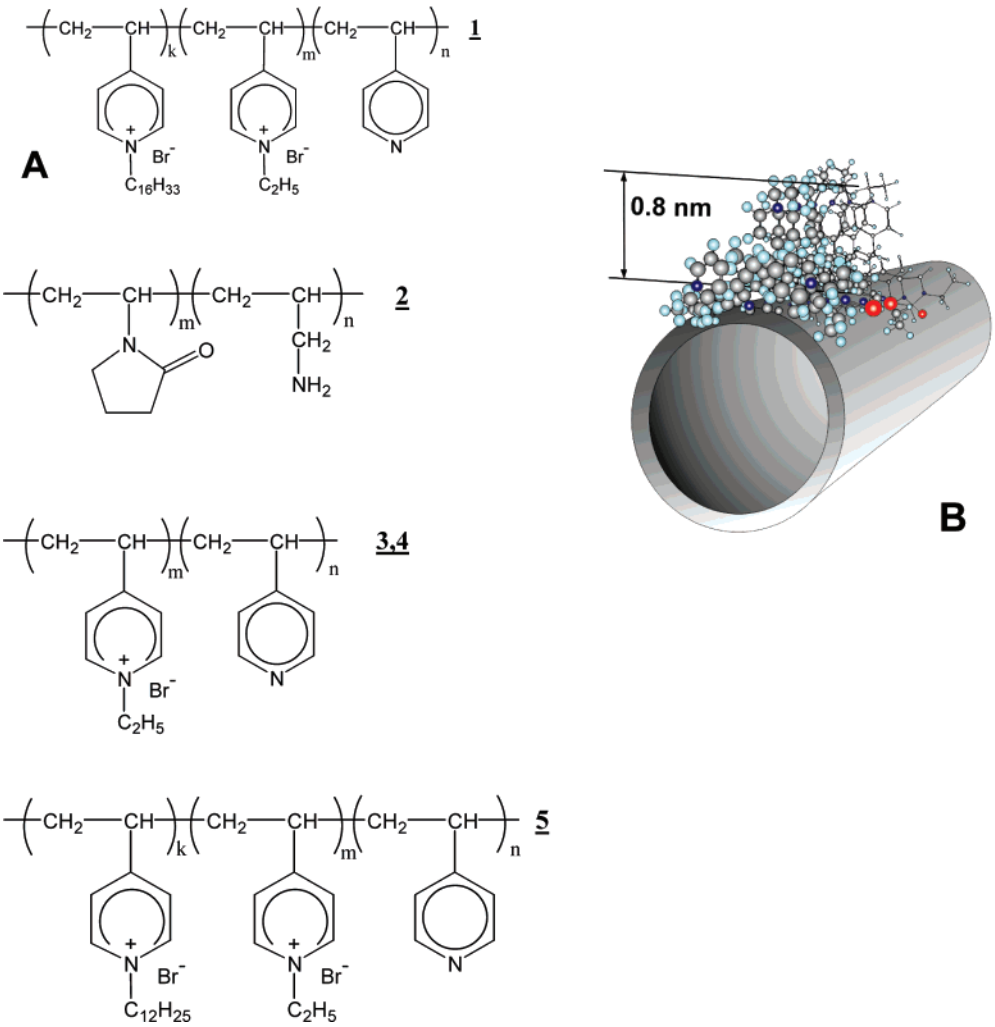

Figure 1. (A) Chemical structures of polymers: Poly(*N*-cetyl-4-vinylpyridinium bromide-*co*-*N*-ethyl-4-vinylpyridinium bromide-*co*- 4-vinylpyridine) (16/75/9) (**1**); poly(vinylpyrro-lidone-*co*-allylamine) (**2**); poly(*N*-ethyl-4-vinylpyridinium bromide-*co*-4-vinylpyridine) (94/6) (**3**); poly(*N*-ethyl-4-vinylpyridinium bromide-*co*-4-vinylpyridine) (30/70) (**4**); poly-(*N*-dodecyl-4-vinylpyridinium bromide-*co*-*N*-ethyl-4-vinylpyridinium bromide-*co*-4-vinyl-pyridine (36/51/13) (**5**). (B) Structural schematics of the adsorption layer of polymer **1** on SWNTs (also see Figure 6). Hydrophobic alkyl radicals in the side chains are omitted for clarity; their position is denoted by red spheres. Color coding of atoms: C, gray; H, light blue; N, purple. Hydrophilic part of the layer is facing the aqueous surrounding, while hydrophobic backbone is lying on the graphite wall. The schematics are hypothetical; the actual positions of the atoms and side groups are not known. CS ChemDraw Ultra 5.0 was used to prepare the 3D image of polymer **1** on SWNTs.

(4-vinylpyridine) (PVP) fraction with a degree of polymerization about 1100 was prepared and then sequentially quaternized with ethyl and cetyl bromides as described before.[43,44] A hydrophobized cationic copolymer, poly(*N*-cetyl-4-vinylpyridinium bromide-*co*-*N*-ethyl-4-vinylpyridinium bromide-*co*-4-vinylpyridine) (16/75/9) (Figure 1, polymer **1**), was thus obtained, with the numbers in parentheses depicting the molar composition of copolymer. Its composition was determined by IR spectroscopy measuring the ratio of intensities at 1600 and 1640 cm^{-1}.[45]

Poly(N-cetyl-4-vinylpyridinium bromide-*co*-*N*-ethyl-4-vinylpyridinium bromide-*co*-4-vinylpyridine) (25 mg) was put in a vial, and 5 mL of deionized water were added. The sample was left for 2 days for polymer swelling followed by addition of 2 mL of dimethylformamide (DMF) for the complete dissolution of the polymer and formation of a transparent solution. Type II or Type III (0.2 mg or 0.4 mg, respectively) was added to 3 mL of a water/DMF (5/2 v/v) solvents mixture with 75 μL of the obtained polymer solution. The mixture was adjusted to pH 9 with 0.1 M NaOH solution for maximum ionization of the carboxylic surface groups of NTs and sonicated for 5 min in the low-power ultrasonic cleaner FS20 (Fisher Scientific, 70 W, 42 kHz) until a visually homogeneous NT suspension was formed. To prepare the suspensions of other types of NTs, 2.5 mg of NTs Type I in the form of a solid paste containing 5 wt % of SWNT in water (as received from manufacturer, no dispersing agent) or 2.5 mg of MWNTs were used in the procedure mentioned above. Data obtained here indicate that short ultrasonic treatment does not affect the surface of NTs. In all cases, dispersions can also be made without sonication after prolonged vigorous shaking of the mixture.

NTs were also suspended in the presence of four other cationic polymers (Figure 1) to clarify the function of different molecular composition: poly(vinylpyrrolidone-*co*-allylamine) (76/24) (**2**), poly(*N*-ethyl-4-vinylpyridinium bromide-*co*-4-vinylpyridine) (94/6) (**3**), poly(*N*-ethyl-4-vinylpyridinium bromide-*co*-4-vinylpyridine) (30/70) (**4**), and poly(*N*-dodecyl-4-vinylpyridinium bromide-*co*-*N*-ethyl-4-vinylpyridinium bromide-*co*-4-vinylpyridine (36/51/13) (**5**). Polymer **2** was by courtesy of Prof. M. Shtilman from Mendeleev University of Chemical Technology (Moscow, Russia). The other three polymers were synthesized from PVP by the above-mentioned procedure using corresponding alkyl bromides and analyzed with IR spectroscopy.

(43) Fuoss, R. M.; Strauss, U. P. *Journal of Polymer Science* **1948**, *3*, 246−263.
(44) Yaroslavov, A. A.; Yaroslavova, E. G.; Rakhnyanskaya, A. A.; Menger, F. M.; Kabanov, V. A. *Colloids and Surfaces, B: Biointerfaces* **1999**, *16*, 29−43.
(45) Kirsh, Y.; Pluzhnov, S. K.; Shomina, T. S.; Kabanov, V. A.; Kargin, V. A. *Vysokomolekulyarnye Soedineniya, Seriya A* **1970**, *12*, 186−204.

2.3. Atomic Force Microscopy Measurements. Atomic force microscopy (AFM) imaging was performed by Nanoscope III (Digital Instruments/Veeco Metrology Group, USA). AFM images were obtained in tapping mode with standard Si/N tips. A silicon substrate was first covered with poly(dimethyldiallylammonium chloride) (PDDA, MW$\approx$ 400 000−500 000; Aldrich) by dipping it in 1 wt % water solution at pH 6.0 for 10 min. After a 3 min wash in deionized water, the substrate was dipped in 1 wt % water solution of poly(acrylic acid (PAA, MW $\approx$ 250 000; Aldrich), pH 6.0, for 10 min. This produces a smooth substrate with uniformly charged surface. A small drop of a nanotube suspension was placed on the prepared substrate and let dry at room temperature, followed by AFM imaging. We found experimentally that PDDA/PAA cushion put on a substrate for AFM imaging makes the surface very hydrophilic and results in more uniform spreading of water droplets containing nanotubes. This provides more appropriate conditions for imaging and gives more accurate representation of nanotube bundling.

2.4. Transmission Electron Microscopy. The high-resolution TEM measurements were carried out using a JEOL 2010F analytical electron microscope with a field emission source. The accelerating voltage was 200 kV. One drop of NT suspension was placed on a copper grid, and an excess of NT suspension was removed. Sample was used after drying at room temperature.

2.5. Dynamic Light Scattering Measurements. The light scattering measurements were done using Nanosizer (HPPS 5001, Malvern Instruments Ltd., UK) equipped with a standard 633 nm laser.

2.6. Electrophoretic Light Scattering Measurements. The zeta potential of the NTs suspensions was measured with a Nicomp 380/ZLS (Particle Sizing Systems, USA). Nanoshere size standard (200 nm, Duke Scientific Corporation, USA) was used as a standard. The group of Dr. James Baker in the University of Michigan Medical School is acknowledged for the use of their Nicomp 380/ZLS particle sizing system.

2.7. UV/vis Absorption Measurements. UV−vis absorption measurements were taken using a Hewlett-Packard HP8453A diode array spectrophotometer.

2.8. Raman Measurements. The Raman characterization was carried out with Types I, II, and III NTs. Their thin film samples were formed by drop coating on a clean silicon wafer with a 25−35 μL of NT suspension and drying at 80 °C on a silicon wafer substrate. This process was repeated for each sample at least 10 times to give a thick film. For each NT type, at least two different samples of unmodified and copolymer **1**-modified NTs were prepared. The Raman measurements were then carried out on a Jobin Yvon microRaman system (Ramanor U1000, Instruments SA, USA) using a spectra-physics Ar ion laser at an excitation wavelength of 514.5 nm (2.41 eV). The backscattered data were analyzed using a double-gating spectrometer and collected using a Hamamatsu photomultiplier (R 943-02, Hamamatsu, USA). All measurements were taken at room temperature, and for each sample the Raman data were collected at different light spots on the sample surface. For every Raman spectrum taken, the position of the peaks was verified by calibrating the spectral positions in respect to silicon substrate peak seen at 521 cm^{-1}.

3. Results and Discussion

The purpose of this study was to prepare positively charged stable suspensions of carbon nanotubes in water and/or mixed polar solvents. Additionally, we wanted this method to be fairly universal, i.e., applicable to NTs from different manufacturers. Irreproducibility of the results obtained with NTs made by various companies represents one of the most significant issues currently present in field of carbon nanostructures. Therefore, SWNT made by three different producers and an MWNT sample from another producer were used in this work following identical procedure of dispersing.

NTs have an exceptionally strong tendency to aggregate in aqueous solutions due to high surface energy, which makes it difficult to suspend them in liquids and to prevent formation of large bundles.[46] To achieve colloidal stability, surfactants for this task have to encapsulate and separate NTs, which necessitates the presence of strong interactions between the graphene sheets and a dispersing agent.[36] The strength of intermolecular interactions should also be combined with its hydrophilicity, at least partially. Traditional surfactants, such as sodium dodecyl sulfate, sodium dodecylbenzenesulfonate, sodium *n*-lauroylsarcosinate, satisfy these requirements and provide stable NT dispersions. However, these dispersions are formed only when these surfactants are present in very high concentrations,[47−49] which is often undesirable for subsequent nanotube processing. Significant improvement of the dispersion efficiency can be obtained with polymeric agents.[50−54] Overall, the efficiency of solubilization increases in most cases as the surfactant or polymer molecular weight increases.

The separation of individual NTs from each other is an exceptionally important task for all carbon nanotechnology. The high polarizability of the π-electrons of graphene sheets leads to powerful van der Waals attraction forces. Structuring of water around the hydrophobic stem produces a large increase of entropy in the system. Altogether these effects result in strong hydrophobic interactions between NTs and subsequent bundling. The high attractive energy between NTs is also related to their axial geometry, which provides a large area of contact. To effectively disperse the bundles, a surfactant with similar interaction makeup is required. One can hypothesize that the amphiphilic properties of the dispersion agent should be augmented by topological resemblance to the NTs.

To prepare positively charged dispersions, one can use amphiphilic cationic polymer molecules with alkyl pendant groups. The hydrophobic alkyl pendant groups of the polymer can provide the binding with the hydrophobic surface of NTs, while the positive charges of polymer molecules will provide compatibility with polar solvent media and prevent their aggregation due to electrostatic repulsion. Additionally, charged polymer molecules can form similar rodlike structures (especially in highly charged states) with axial geometry and, therefore, can potentially mimic and replace individual nanotubes in the bundles. Five polymers with different hydrophobic and hydrophilic parts were synthesized and examined as nanotube dispersing agents (Figure 1). They combine hydrophobic backbone and hydrophilic side chains or vice versa. The

(46) Zhang, N.; Xie, J.; Guers, M.; Varadan, V. K. *Smart Materials and Structures* **2003**, *12*, 260−263.
(47) Moore, V. C.; Strano, M. S.; Haroz, E. H.; Hauge, R. H.; Smalley, R. E.; Schmidt, J.; Talmon, Y. *Nano Letters* **2003**, *3*, 1379−1382.
(48) Jin, Z. X.; Goh, S. H.; Xu, G. Q.; Park, Y. W. *Synthetic Metals* **2003**, *135−136*, 735−736.
(49) Islam, M. F.; Rojas, E.; Bergey, D. M.; Johnson, A. T.; Yodh, A. G. *Nano Letters* **2003**, *3*, 269−273.
(50) Star, A.; Steuerman, D. W.; Heath, J. R.; Stoddart, J. F. *Angewandte Chemie, International Edition* **2002**, *41*, 2508−2512.
(51) Star, A.; Stoddart, J. F.; Steuerman, D.; Diehl, M.; Boukai, A.; Wong, E. W.; Yang, X.; Chung, S. W.; Choi, H.; Heath, J. R. *Angewandte Chemie, International Edition* **2001**, *40*, 1721−1725.
(52) Maser, W. K.; Benito, A. M.; Callejas, M. A.; Seeger, T.; Martinez, M. T.; Schreiber, J.; Muszynski, J.; Chauvet, O.; Osvath, Z.; Koos, A. A.; Biro, L. P. *Materials Science & Engineering, C: Biomimetic and Supramolecular Systems* **2003**, *C23*, 87−91.
(53) Nativ-Roth, E.; Levi-Kalisman, Y.; Regev, O.; Yerushalmi-Rozen, R. *Journal of Polymer Engineering* **2002**, *22*, 353−368.
(54) Zengin, H.; Zhou, W.; Jin, J.; Czerw, R.; Smith, D. W., Jr.; Echegoyen, L.; Carroll, D. L.; Foulger, S. H.; Ballato, J. *Advanced Materials (Weinheim, Germany)* **2002**, *14*, 1480−1483.

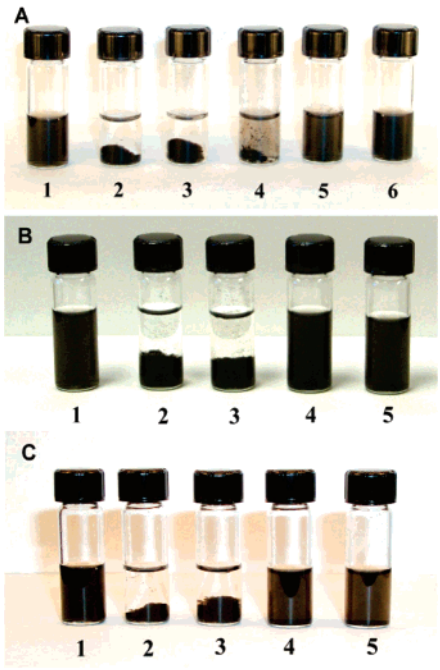

Figure 2. Suspensions of (A) SWNTs (Nanocyl, Belgium) (1, 2, 3, 4, 5) and MWNTs (Nano-Lab, USA) (6); (B) SWNTs (Buckytubes, CNI, USA); **(**C) SWNTs (SWeNT, SouthWest Nanotechnologies, USA) after 4 days after agitation prepared with different polymeric dispersing agents. For vials 1−5, the number of the vial corresponds to the number of the polymer agent in Figure 1. (1) Poly(*N*-cetyl-4-vinylpyridinium bromide-*co*-*N*-ethyl-4-vinylpyridinium bromide-*co*-4-vinylpyridine) (16/75/9); (2) poly(vinylpyrrolidone-*co*-allylamine); (3) poly(*N*-ethyl-4-vinylpyridinium bromide-*co*-4-vinylpyridine) (94/6); (4) Poly(*N*-ethyl-4-vinylpyridinium bromide-*co*-4-vinylpyridine) (30/70); (5) poly(*N*-dodecyl-4-vinylpyridinium bromide-*co*-*N*-ethyl-4-vinylpyridinium bromide-*co*-4-vinylpyridine (36/51/13); (6) MWNT with polymer **1**, i.e., poly(*N*-cetyl-4-vinylpyridinium bromide-*co*-*N*-ethyl-4-vinylpyridinium bromide-*co*-4-vinylpyridine) (16/75/9).

Table 1. Average Size of Single-Wall Carbon Nanotubes Determined from Light Scattering Assuming Rodlike Shape of the Particles

	effective diameter of particles in SWNT dispersions obtained by light scattering, nm		
polymer	type I (Nanocyl)	type II (BuckyPearls)	type III (SWeNT)
1	400	850	450
4		2580	670
5	550	1490	510

hydrophilic−hydrophobic balance in the macromolecules can be varied by different degrees of substitution and/or by different natures of substitutes in the side chain.

The dispersion procedure was identical for all the polymers in Figure 1. For polymers **1** and **5**, no NT precipitation was observed for at least several weeks (Figure 2). For polymer **1**, most of the carbon material remained suspended for over a year since the dispersions were made (Figure 2). Polymers **2**, **3**, and **4** did not give stable NT dispersions; phase separation and formation of rough sediments were observed for them (Figure 2). For this reason, most of the characterization methods were applied to dispersions made on the basis of polymers **1** and **5**. Effective particle size in dispersions measured by light scattering in suspension assuming their rigid rodlike geometry was between 400 and 670 nm (Table 1) for Type I and Type III NTs stabilized with **1** and **5**, respectively. This is very close to the expected length of SWNT. The light-scattering data gave consistently higher sizes for Type II NTs (Table 1), which most likely was related to a greater starting length of the tubes or slightly greater percentage of the bundles (see below).

According to AFM data (Figure 3), most of the NTs in polymer-**1**-stabilized suspension have a length from 350 to 500 nm (Figure 3A), which correlates well with the results of light scattering. Most importantly, analysis of multiple AFM images indicates that the majority of SWNTs are present as single tubes (Figure 3A), which can be seen from the section analysis of the corresponding AFM image: the height of the NT-like objects does not exceed 1.5 nm, which is very close to the specifications of the NT diameter from the corresponding manufacturer (1.3−1.5 nm for Type I) and smaller than the expected diameter of the bundles. While formation of colloidal dispersion of single SWNT in aqueous media was also observed for some other polymers,[34] polymer **1** demonstrates dominance of single tubes in the dispersion. Only a small fraction (a single instance in more than 10 images similar to Figure 3A) of NTs clearly exists as bundles with a diameter of 10−15 nm. To compare with other data on SWNTs solubilized in aqueous media, this is close to the average diameter of bundles prepared by solubilization of NTs in solution of low molecular weight surfactants;[49] however, their concentration was 10−20 times higher than that of polymer **1**. The diameters of the bundles here are smaller than the size of the bundles observed in dispersions made with the help of surfactant−polymer mixture PVA/PVP/SDS, i.e. 30 nm,[35] or oxidation according to existing procedures by an acidic $KMnO_4$ and following functionalization with Wilkinson's complex, i.e., 15−20 nm in diameter.[55]

For polymer **5**, single nanotubes still dominate; however, one can also observe a significant amount of spherical objects with a mean diameter of about 100 nm (Figure 3B). The latter probably corresponds to polymer micelles formed by several **5** macromolecules, which was substantiated by observation of enhanced scattering in the polymer-**5** solution using Malvern Nanosizer. Similar micelles but smaller in size and quantity may form for polymer **1** as well (Figure 3A).

It is important to note that the same polymer **1** worked quite well not only for SWNTs but also for MWNTs (Figure 2 and Figure 3C). No NT precipitation was observed from the suspension after 4 days (Figure 2). It can be concluded from AFM images (Figure 3C) that, similarly to SWNTs, MWNTs are also present in the dispersions as single tubes. The manufacturer-specified average diameter of MWNT is 20 nm. This matches very well the diameter of the tubes in dispersion (Figure 3C), which ranges from 15 to 25 nm. No bundles of MWNTs were detected. The fact of high stability dispersions of single MWNT is significant, because it indicates the potential of polymers **1** and **5** as fairly universal solubilizing agent for markedly different NTs.

UV−vis spectra of Type II and Type III dispersions clearly demonstrated van Hove singularities at a wide range of concentrations of SWNTs (Figure 4) or the polymer (Figure 5).[56] The optical spectra of SWNT Type III suspension with polymer **1** have several peaks corresponding to photon energies of 1.2, 1.8, and 2.3 eV (Figures 4, 5) independent of dispersion conditions.

(55) Banerjee, S.; Wong, S. S. *Journal of the American Chemical Society* **2002**, *124*, 8940−8948.
(56) van Hove, L. *Physical Review* **1953**, *89*, 1189−1193.

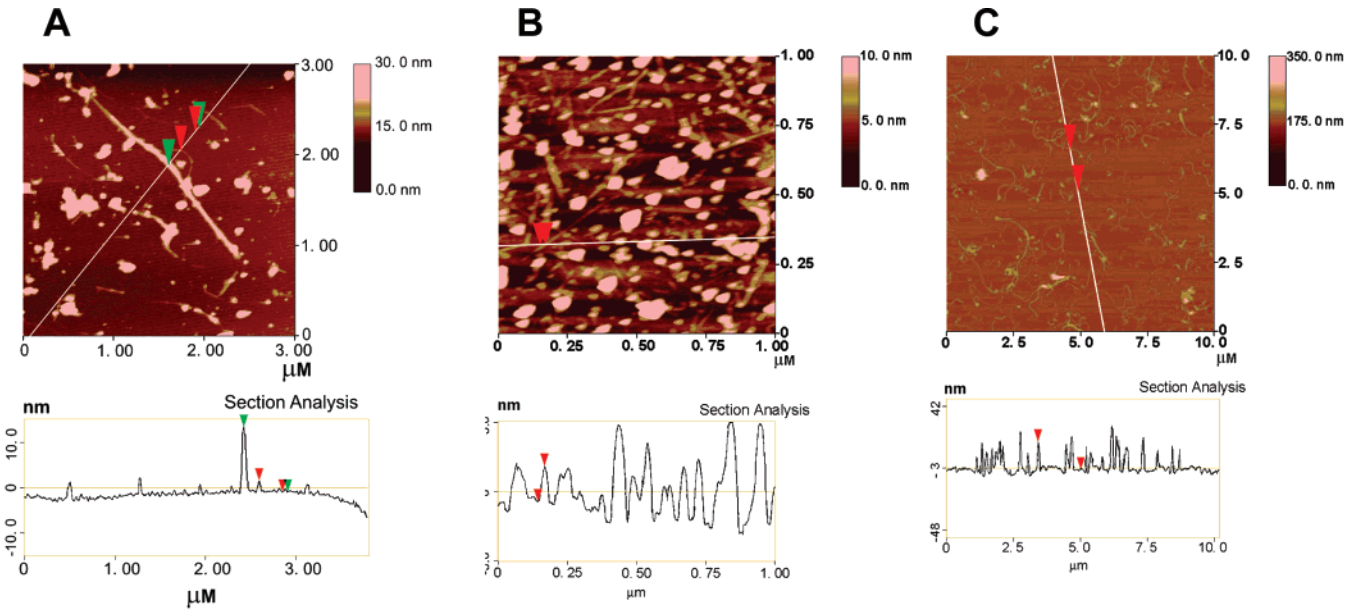

Figure 3. AFM investigation of nanotube dispersions stabilized by polymers deposited on Si substrates. (A) Dispersions of SWNTs, Type I, modified with polymer **1**. (B) Dispersions of SWNTs, Type I, modified with polymer **5**. (C) Dispersions of MWNT modified with polymer **1**.

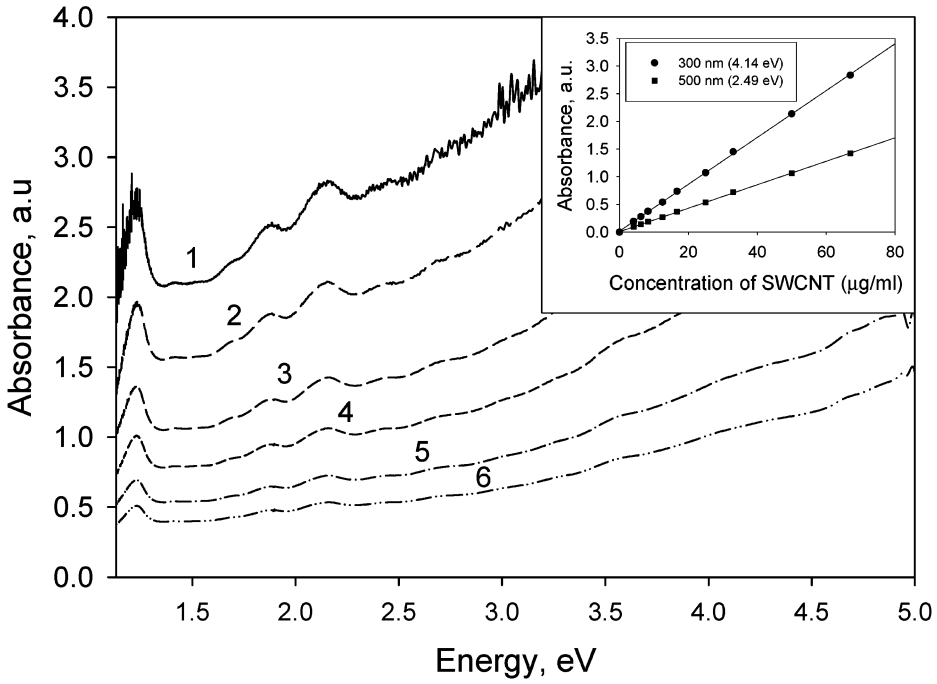

Figure 4. UV−vis absorption spectra of polymer-**1**-stabilized SWNTs (SWeNT, Type III) suspension of different concentrations: (1) 0.133 mg/mL; (2) 0.1 mg/mL; (3) 0.067 mg/mL; (4) 0.05 mg/mL; (5) 0.033 mg/mL; (6) 0.025 mg/mL; and concentration dependencies of the absorbance at two wavelength values, 300 nm (4.14 eV) and 500 nm (2.49 eV) (inset).

All these peaks are well-known and identified for pristine SWNTs.[57−58] The transition at 1.2 eV is assigned to the second pair of singularities $\nu_s^2 \rightarrow c_s^2$ of semiconducting nanotubes. The absorption band at 1.8 eV can correspond to the first pair of singularities of metallic nanotubes. As reported in refs 59 and 60[59,60], these features disappear when the graphene surface is covalently modified, which can be seen, for instance, in UV−vis spectra of partially oxidized Type I SWNTs (Supporting Information, Figure S1). The observation of very pronounced van Hove singularities here is significant because this fact indicates that the preparation procedure involving polymers **1** or **5** does not result in marked alteration of aromatic system of SWNTs responsible for their unique strength and conductivity. Thus, SWNTs suspended by polymer ***1*** are modified in noncovalent fashion keeping all the features of pristine NTs. The dependence of absorbance on concentration at 300 and 500 nm obeys Beer's law (Figure 4, inset), indicating no effects,

(57) Wildoer, J. W. G.; Venema, L. C.; Rinzier, A. G.; Smalley, R. E.; Dekker, C. *Nature (London)* **1998**, *391*, 59−62.
(58) Jacquemin, R.; Kazaoui, S.; Yu, D.; Hassanien, A.; Minami, N.; Kataura, H.; Achiba, Y. *Synthetic Metals* **2000**, *115*, 283−287.
(59) Bahr, J. L.; Yang, J.; Kosynkin, D. V.; Bronikowski, M. J.; Smalley, R. E.; Tour, J. M. *Journal of the American Chemical Society* **2001**, *123*, 6536−6542.
(60) Strano, M. S.; Dyke, C. A.; Usrey, M. L.; Barone, P. W.; Allen, M. J.; Shan, H.; Kittrell, C.; Hauge, R. H.; Tour, J. M.; Smalley, R. E. *Science (Washington, D.C., United States)* **2003**, *301*, 1519−1522.

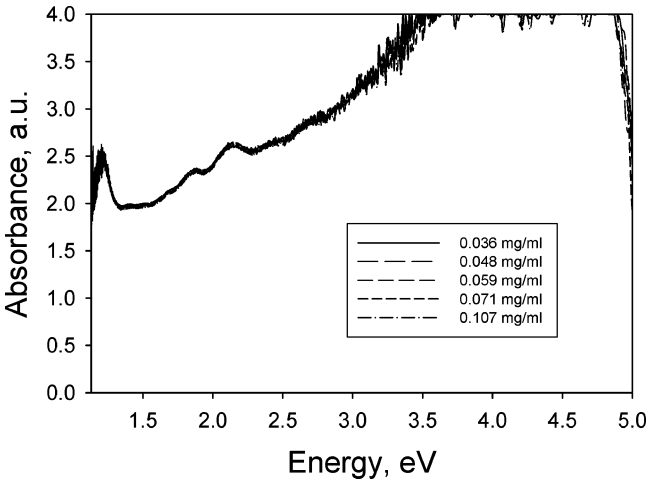

Figure 5. UV−vis spectrum of 0.133 mg/mL Type III SWNTs suspended after addition of various amounts of polymer **1**; each of the NT's suspensions was sonicated during 5 min.

which could be associated with concentration-dependent NT aggregation. Independence of UV−vis spectra of dispersion on polymer concentration (Figure 5) also demonstrates that the observed features are the true peaks from nanotubes rather than a possible charge-transfer complex, which often have bands in the same region.

The single-tube nature of the SWNT dispersions can also be confirmed by TEM images (Figure 6). Moreover, it can be clearly seen how uniformly the polymer layer coats the SWNT surface, which is apparently the reason for the stability of the dispersions and their single-tube nature. As seen on TEM images (Figure 6), the thickness of polymer layer self-assembling onto the SWNT surface is about 1−1.5 nm. It correlates well with the thickness of a polymer **1** monolayer taking into account the bulky alkyl substitute in side chain of polymer molecule. On the basis of molecular geometry and assuming the placement of hydrophobic backbone directly on along the graphite surface (Figure 1B), the approximate thickness of the polymer layer can be estimated to be 0.8 nm. The diameter of individual SWNTs, Type I is equal 1.3−1.5 nm as seen in Figure 6, which is in a good agreement with data obtained from the manufacturer, i.e. 1−2 nm (Figure 2A,B). These images also afford direct measurements of the diameter of the SWNT with the polymer layer on it. The total diameter of the coated tube is 3.3−3.5 nm. Interestingly, the apparent diameter of the NTs determined from AFM section analysis is 1.5 nm. This discrepancy is related to the difference in the imaging techniques. Since the difference in physical strength of the polymer coating and the carbon core is very significant, the sharp end of the scanning probe is likely to cause the deformation in the polymer layer, pushing it aside when the sample of coated SWNT is scanned in tapping mode AFM. This makes an AFM thickness data to be close to the true diameter of the graphite roll. This effect should be taken into account in other systems as well to avoid inadvertent underestimation of the true diameter of the coated NTs.

Effect of uniform coating of the NTs by the designed polymer can also be seen in electrophoretic characteristics of the colloid, such as zeta potential. At any pH, the zeta potential of SWNT and MWNT is positive. It does not change too much from strongly acidic to strongly basic media (Tables 2 and 3), which is the expected behavior for quaternized ammonium moieties (Figure 1) determining the surface charge in the coated NTs.

Once we know the structure of the polymer−NT complex, it would be instructively useful to discuss the difference that polymer composition makes for NT dispersion. All the polymers in Figure 1 have similar functionalities: a hydrophobic part, a hydrophilic part, and a positively charged headgroup. Given the fact that only polymers **1** and **5** displayed efficient solubilization of NTs, it is important to rationalize this observation so that the search for new (potentially multifunctional) dispersing agents can be continued with a greater degree of certainty. There are two chemically different hydrophobic sites in polymer **1**: in the chains and in the backbone (Figure 1). Both of them can have potentially strong hydrophobic interactions with the graphite surface, which was most likely essential in determining its performance here. The aromatic groups, which also carry the charge, are located closer to the backbone. This increases their affinity to the highly conjugated graphene surface and efficiency of debundling. The failure of polymers **3** and **4** to disperse the nanotubes indicates that the hydrophobic interactions in the side chains are probably most important for the preparation of stable suspensions.

The content of hydrophobic fragments in polyampholyte macromolecules and their arrangement within macromolecule seem to be extremely important for stabilizing nanotubes. Polymer **5**, with a high content of pendant alkyl groups, forms intra- and intermolecular micelles, which are likely to persist in solution after adding nanotubes. Polymer **4**, with hydrophobic units in the backbone, is unable to stabilize nanotubes apparently due to weak binding to the surface. This is indirectly corroborated by the absence of solubilization effect in the case of cationic polymer **3** with limited hydrophobicity and cationic copolymer **2**.

The strength of adherence of the polymer chains to the surface of NTs via hydrophobic interaction can also be seen from Raman spectra. The presence of the polymer coating substantially affects the vibration frequencies of both radial and tangential movement of the carbon atoms, which is indicative of strong attractive forces between the macromolecule and the graphite sheet. Figure 7 shows the Raman spectra of pristine and polymer-**1**-coated samples averaged over several scans. Both spectra show similar spectral patterns. Peaks arising from the radial motion of the carbon atoms, i.e., the radial breathing modes (RBM),[61,62] are seen in the 100−300 cm^{-1} range. Many peaks are seen within this range, which indicates the presence of a wide distribution of SWNT diameters in the dispersions.[63,64] Using the well-known relation between the RBM band frequency and the diameter of the nanotubes[58]

$$\nu_{RBM} = 238/d^{0.93}$$

where ν_{RBM} is the RBM frequency in cm^{-1}, and d is the tube diameter in nm, one can calculate the diameter of the nanotubes

(61) Rao, A. M.; Richter, E.; Bandow, S.; Chase, B.; Eklund, P. C.; Williams, K. A.; Fang, S.; Subbaswamy, K. R.; Menon, M.; Thess, A.; Smalley, R. E.; Dresselhaus, G.; Dresselhaus, M. S. *Science (Washington, D.C.)* **1997**, *275*, 187−191.
(62) Sauvajol, J. L.; Anglaret, E.; Rols, S.; Alvarez, L. *Carbon* **2002**, *40*, 1697−1714.
(63) Alvarez, L.; Righi, A.; Rols, S.; Anglaret, E.; Sauvajol, J. L.; Munoz, E.; Maser, W. K.; Benito, A. M.; Martinez, M. T.; de la Fuente, G. F. *Physical Review B: Condensed Matter and Materials Physics* **2001**, *63*, 153401-1-153401/4.
(64) Kuzmany, H.; Plank, W.; Hulman, M.; Kramberger, C.; Gruneis, A.; Pichler, T.; Peterlik, H.; Kataura, H.; Achiba, Y. *European Physical Journal B: Condensed Matter Physics* **2001**, *22*, 307−320.

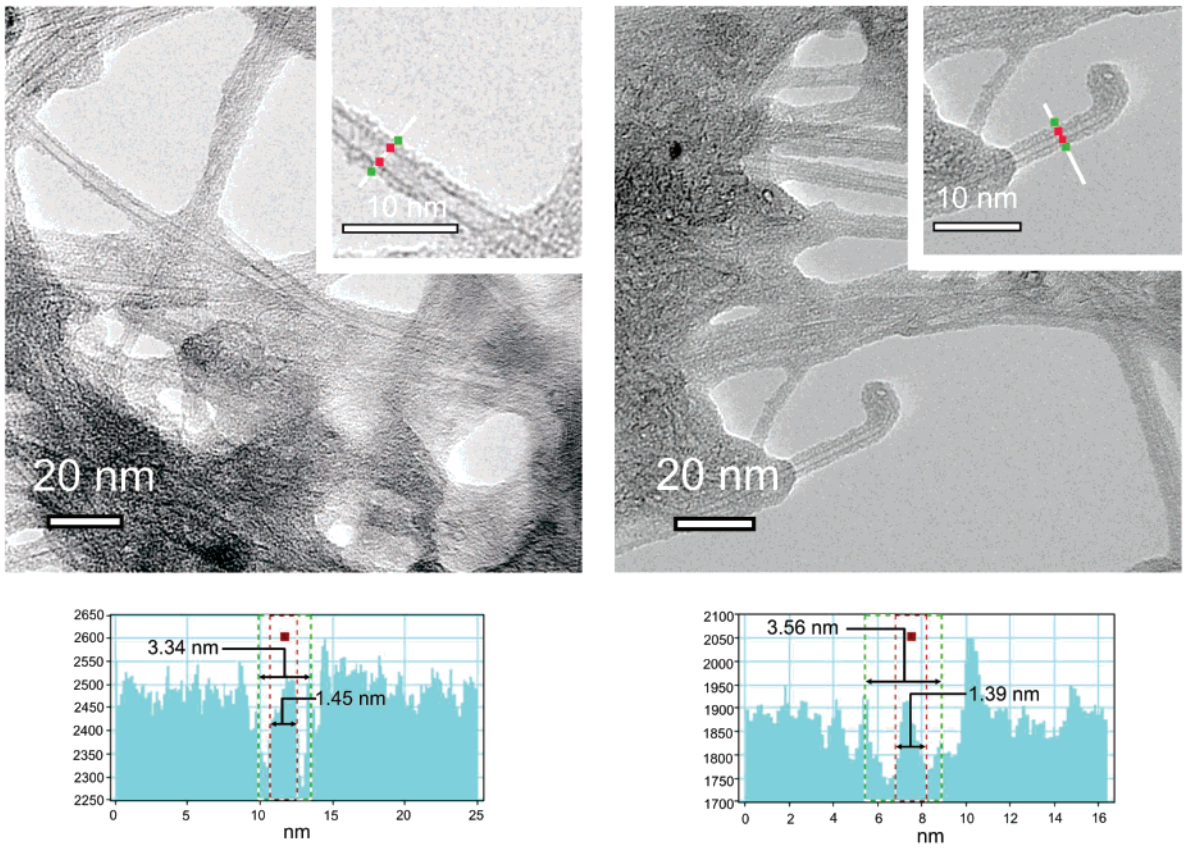

Figure 6. TEM images of Type I SWNTs (Nanocyl) stabilized by polymer **1**; ratio SWNT/polymer is 1.5/1 by weight.

Table 2. Zeta Potential vs pH for Suspension of SWNTs, Type I, in Water/DMF (5/2 v/v) Solution at Temperature 25 °C

pH	12	10	8	7	6.5	5.5	4.5	4	3
zeta potential, mV ±3 mV	16	20	22	22	24	25	25	26	26

Table 3. Zeta Potential vs pH for Suspension of MWNTs in Water/DMF (5/2 v/v) Solution at Temperature 25 °C

pH	12	10	8	7	6.5	5.5	4.5	4	3
zeta potential, mV ±3 mV	13	22	24	25	24	24	26	25	28

corresponding to the dominant RBM bands seen for the different types of nanotubes used. The RBM peaks with the highest frequency in the pristine uncoated samples correspond to SWNTs with a diameter of 1.3 nm (corresponding to the RBM at ca. 182 cm^{-1}) for Type I, 0.9 nm (corresponding to the RBM at ca. 262 cm^{-1}) for Type II, and 0.9 nm (corresponding to the RBM at ca. 263 cm^{-1}) for Type III (Figure 5, insets). (Figure 7 inserts). The band seen in the 1500−1600 cm^{-1} region is the so-called G-band resulting from the tangential C−C stretching vibrations both longitudinally and transversally on the NT axis.[65] The shape of this G-band has been known to differ with the electronic identity of NTs depending whether they are metallic or semiconducting.[66]

The disorder peak, also known as the D-band, can be found in the 1300−1400 cm^{-1} region. This peak is attributed to scattering from sp^2 carbons containing defects. The strength of this peak is related to the amount of disordered graphite and the degree of conjugation disruption in the graphene sheet.[66]

Despite all the different diameters of SWNTs in the samples and various manufacturers, the whole set of all RBM peaks for Type I, II, and III NTs shifts to higher Raman frequencies when they are coated with polymer **1** by approximately the same value (Figure 7). As such, the dominant RBM peak in the pristine sample of Type I NTs is observed at 182 cm^{-1}, while the corresponding peak after addition of the polymer is seen at 188 cm^{-1} (Figure 7A inset). A similar change in RBM frequency has been reported for NTs incorporated and coated with different polymers and peptides.[67−69] For Type II NTs, two dominant RBM peaks are seen in the 225−300 cm^{-1} range (Figure 7B inset). Here, the set of RBM bands shift by at least 3 to 4 wavenumbers to higher Raman frequencies in the presence of polymer **1**. The major bands seen in "naked" samples at 245 and 263 cm^{-1} are located at 249 and 267 cm^{-1} in the polymer-coated samples. The same behavior was also observed in the peak positions of the RBM bands of Type III NTs where the upshift in the frequency of Raman RBM modes in the presence of the polymer is at least 4−6 wavenumbers (Figure 7C inset).

A clear trend in the spectral position of the G-band before and after the modification with polymer **1** can also be noticed. In the spectra of pristine samples of Type I, II, and III SWNTs, the G-band is peaking in the 1583−1589 cm^{-1} range, while, in

(65) Kukovecz, A.; Kramberger, C.; Georgakilas, V.; Prato, M.; Kuzmany, H. *European Physical Journal B: Condensed Matter Physics* **2002**, *28*, 223−230.
(66) Dresselhaus, M. S.; Dresselhaus, G.; Jorio, A.; Souza Filho, A. G.; Saito, R. *Carbon* **2002**, *40*, 2043−2061.
(67) Dalton, A. B.; Stephan, C.; Coleman, J. N.; McCarthy, B.; Ajayan, P. M.; Lefrant, S.; Bernier, P.; Blau, W. J.; Byrne, H. J. *Journal of Physical Chemistry B* **2000**, *104*, 10012−10016.
(68) Stephan, C.; Nguyen, T. P.; de la Chapelle, M. L.; Lefrant, S.; Journet, C.; Bernier, P. *Synthetic Metals* **2000**, *108*, 139−149.
(69) Dieckmann, G. R.; Dalton, A. B.; Johnson, P. A.; Razal, J.; Chen, J.; Giordano, G. M.; Munoz, E.; Musselman, I. H.; Baughman, R. H.; Draper, R. K. *Journal of the American Chemical Society* **2003**, *125*, 1770−1777.

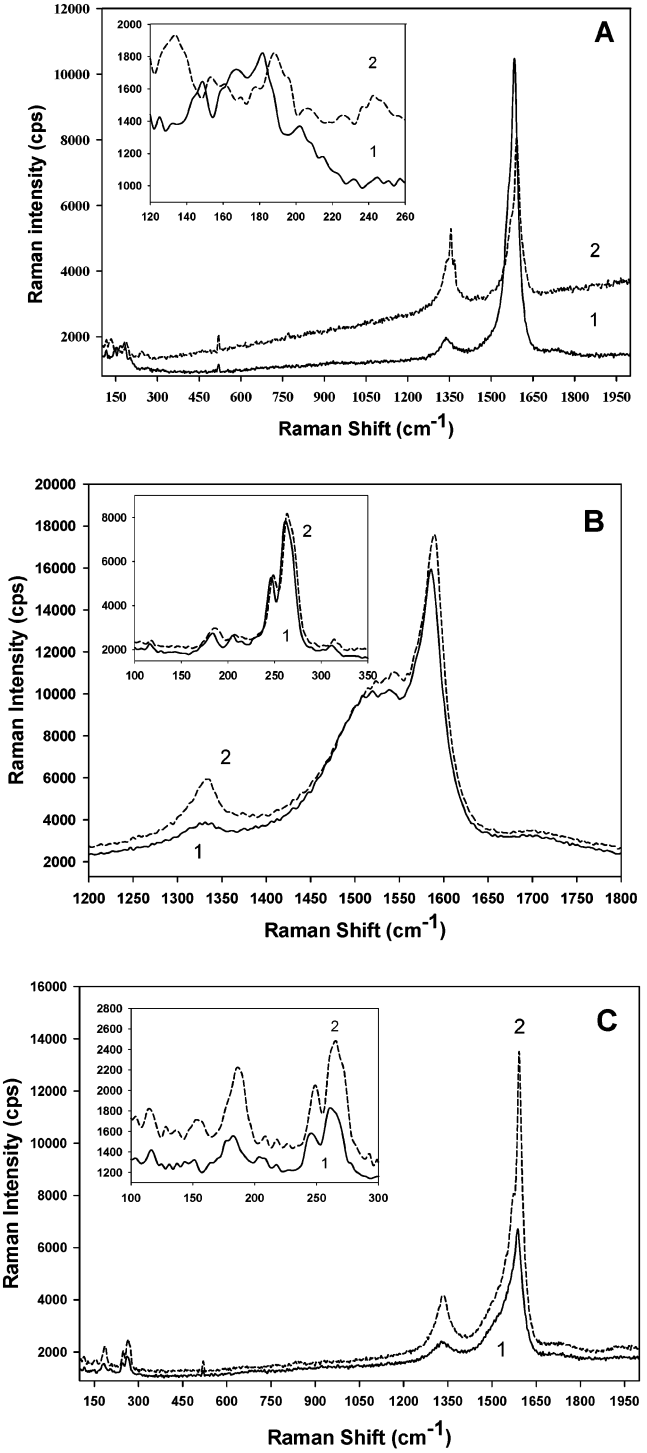

Figure 7. Raman spectra of SWNTs before (plots 1, solid line) and after (plots 2, dashed line) modification with polymer **1**. (A) Type I; (B) Type II; (C) Type III.

the presence of polymer, this band is seen to shift to higher wavenumbers (Figure 7) similarly to the RBM frequencies. The most evident shift is seen in Type I SWNTs, where the G-band shifts by 9 cm^{-1} from 1583 to 1592 cm^{-1} (Figure 7A). Types II and III SWNTs display a significantly smaller (around 3 cm^{-1}) shift in the G-band (Figure 7A and B).

By inspecting the 1300−1400 cm^{-1} spectral range where the D-band is appearing, we noticed some changes in the intensity and sharpness of this D-band as the polymer coating around NTs is formed, while its spectral shift is insignificant. For Type I SWNTs, a sharp increase in the D-band intensity as well as the ratio of the D-band to that of the G-band intensity should be noted (Figure 7A). An increase in the intensity and sharpness of the D-band, but not necessarily the D-band to G-band intensity ratio, was also seen in the polymer Raman spectra of both Types II and III SWNTs (Figure 7B and C).

The observed changes in the Raman spectra can be explained by considering wrapping of the polymers around SWNTs in the fashion presented in Figure 6. The strong attachment of the polymer to NTs results in the observed upshift of the RBM and G-band peaks due to increase in the elastic constant of the harmonic oscillator of the polymer-coated SWNT. The hydrophobic and van der Waals attraction forces between the polymer and the graphite sheet increase the energy necessary for vibrations to occur, which is reflected in the higher frequency of Raman peaks. One should also point out that the spectral shift of the peaks is fairly uniform for SWNTs of all diameters in the samples, which can be seen particularly well for RBMs (Figure 7, all inserts). Also, there is no line broadening of RBM; even a slight line narrowing of the G-band is observed. These two facts are indicative of the homogeneity of the polymer **1** layer around different SWNTs. Its thickness of 0.8−1.0 nm is apparently a fairly consistent property for all colloid particles of **1**-modified SWNTs.

The position of the D-band and D/G-band intensity ratio typically changes when covalent modification of the graphene sheet occurs.[70−72] The data presented above indicate that the polymers used here do not covalently attach to the NTs (Figures 4, 5). The small increase of the D-band and D/G ratio can be potentially attributed to three processes. (1) Besides nanotubes, the polymer coating can also form on remaining carbon particles responsible for the appearance of D-band. This results in their disaggregation and therefore stronger Raman signal from them. (2) The polymer coating causes field disturbance and physical strain in the graphite skeleton,[73] which make excitation of these D-vibrations in the nonlinear Raman scattering process more efficient. Such property can be foreseen from the coupling mechanism of the vibrations of the dipole in the virtual excited state with lattice vibrations of the graphene sheet.[77] The evidence of sensitivity of D-band to strain in graphene skeleton can be also seen by the gradual shift of its wavelength in response to axial stretching as reported by X. Zhang in ref 35. (3) The short (5 min) and low power sonication treatment used to disperse nanotubes may cause some damage to the grapheme sheet, which shows up as an enhancement of the D-band. At the

(70) Bahr, J. L.; Tour, J. M. *Chemistry of Materials* **2001**, *13*, 3823−3824.
(71) Dyke, C. A.; Tour, J. M. *Nano Letters* **2003**, *3*, 1215−1218.
(72) Dyke, C. A.; Tour, J. M. *Journal of the American Chemical Society* **2003**, *125*, 1156−1157. Brown, S. D. M.; Jorio, A.; Dresselhaus, M. S.; Dresselhaus, G. *Physical Review B* **2001**, *64*, 073403. Pimenta, M. A.; Jorio, A.; Brown, S. D. M.; Souza Filho, A. G., Dresselhaus, G.; Hafner, J. H.; Lieber, C. M.; Saito, R.; Dresselhaus, M. S. *Physical Review B* **2001**, *64*, 041401.
(73) Caruso, F. *Advanced Materials (Weinheim, Germany)* **2001**, *13*, 11−22.
(74) Caruso, F.; Sukhorukov, G. *Coated colloids: preparation, characterization, assembly and utilization*; Max Planck Institute of Colloids and Interfaces: Potsdam, Germany, 2003. Kotov, N. A. Ordered Layered Assemblies of Nanoparticles. *MRS Bulletin* **2001**, *26* (12), 992.
(75) Rouse, J. H.; Lillehei, P. T. *Nano Letters* **2003**, *3*, 59−62.
(76) Guo, Y.; Minami, N.; Kazaoui, S.; Peng, J.; Yoshida, M.; Miyashita, T. *Physica B: Condensed Matter* **2002**, *323*, 235−236.
(77) Saito, R. Takeya, T.; Kimura, T.; Dresselhaus, G.; Dresselhaus, M. *Physical Review B* **1998**, *57*, 4145. Matthews, M. J.; Pimenta, M. A.; Dresselhaus, G.; Dresselhaus, M. S.; Endo, M. *Physical Review B* **1999**, *59*, R6585. Jishi, R. A.; Venkataraman, L.; Dresselhaus, M. S.; Dresselhaus, G. *Chem. Phys. Lett.* **1993**, *209*, 77.

moment we cannot give preference to any of these hypotheses. We will only note that if (1) is true, it will be easier to separate the admixtures from the nanotubes. If hypothesis (3) is true, then sonication should be replaced with shaking, which also works well for the system described.

4. Conclusions

The hydrophobic interactions mostly with side chains ensure strong binding of the polycation to the NT surface, which is aided by the inherent ability of the macromolecular chains to wind around a rodlike object. This method of NT dispersion is fairly universal because of the excellent control over the hydrophilic−hydrophobic balance and mode of interactions in the comb-polymers due to the variability of the degree of derivatization as well as in the chemical properties of the side chains. For instance, similar suspension, can be obtained with negatively charged amphiphilic polyelectrolytes, which open the way to numerous processing technologies including layer-by-layer deposition.[1,73−76] Importantly, it also preserves the integrity of the graphite sheet, which is critical for many applications. Inclusion of aromatic functional groups can further improve the performance of the polymeric dispersing agent.

Acknowledgment. N.A.K. thanks the financial support of this project from AFOSR, NSF-CAREER, NSF-Biophotonics, NIH-NASA, and OCAST. A.A.Y. thanks OSU for the financial support during his visit. Support for M.K.G. and J.P.W. was supplied in part by an NSF EPSCoR grant. The group of Dr. James Baker in the University of Michigan Medical School is acknowledged for the use of their Nicomp 380/ZLS particle sizing system.

Supporting Information Available: UV−vis absorption spectra of SWN obtained from Nanocyl (Namur, Belgium) (Type I) dispersed with polymer **1** at different concentrations. This material is available free of charge via the Internet at http://pubs.acs.org.

JA045670+